Petroleum Science 23 (2026) 4100–4112

Contents lists available at ScienceDirect

Petroleum Science

journal homepage: www.keaipublishing.com/en/journals/petroleum-science

Original Paper

Experimental investigations on spontaneous imbibition process applied in tight conglomerate oil reservoir

Xiang Zhou [a,b,*], Zhong-Wen Hu [a], Feng Wang [c], Zhao-Wen Jiang [c], Yu-Long Zhao [a,b], Tao Zhang [a,b], Lie-Hui Zhang [a], Qi Jiang [a]

[a] *Petroleum Engineering School, Southwest Petroleum University, Chengdu, 610500, Sichuan, China*
[b] *State Key Laboratory of Oil and Gas Reservoir Geology and Exploitation, Southwest Petroleum University, Chengdu, 610500, Sichuan, China*
[c] *Research Institute of Exploration and Development, Xinjiang Oilfield Company, PetroChina, Karamay, 834000, Xinjiang, China*

A R T I C L E I N F O

Article history:
Received 26 October 2025
Received in revised form
24 December 2025
Accepted 25 February 2026
Available online 27 February 2026

Edited by Meng-Jiao Zhou

Keywords:
Spontaneous imbibition
Pore and throat size
Tight conglomerate
Surfactant solution
NMR

A B S T R A C T

In this research, experimental studies were conducted to investigate the influences of permeability and surfactant solution on varying permeability cores in the spontaneous imbibition process. Totally, four types of experiments were implemented, namely, measurements of pore-throat distribution, contact angle, interfacial tension and lower limits of pore and throat size. The experimental results reveal significant variations in pore-throat size across the cores, ranging from as low as 0.61 nm to as high as 70.58 μm in the targeted core. With increasing concentration of surfactant solution, both the contact angle and interfacial tension decreased. Compared with formation water, the contact angle decreased from 48.36° to 23.75°and interfacial tension decreased from 23.92 to 9.69 mN/m for the surfactant solution injection with the optimized concentration of 0.20%. Experiments of spontaneous imbibition indicates that the imbibition process was dominated by the initial stage across all cores. The highest imbibition efficiency occurred in macropore (>10 μm) for cores #4 and #5 with low permeability. Mesopores (1 to 10 μm) consistently showed the highest contribution to oil production, confirming their central role in the tight conglomerate reservoir. With varying injection media, the lower limits of pore and throat size was measured using Nuclear Magnetic Resonance, and significant reduction from water phase to surfactant solution phase was investigated. Therefore, the oil recovery factor can be enhanced in the surfactant solution injection process. The findings can be used to predict the effect of permeability and surfactant solution on the tight conglomerate oil recovery process.
© 2026 The Authors. Publishing services by Elsevier B.V. on behalf of KeAi Communications Co. Ltd. This is an open access article under the CC BY license (http://creativecommons.org/licenses/by/4.0/).

1. Introduction

Nowadays, tight oil reserves are increasingly focused on by the scholars, because of the continuous depletion of conventional oil reserves (Le Van et al., 2025; Tang et al., 2019; Zhou et al., 2019, 2025). When water-based recovery approaches are applied in the tight oil reservoirs, the low permeability remarkable amplifies the role of capillary pressure, which becomes a dominant driving force for spontaneous imbibition (Zheng et al., 2021). The imbibition process affects the oil flow dynamics in tight formation significantly (Liu et al., 2024; Xiao et al., 2025). Both experimental studies and pilot tests have proved that, spontaneous imbibition approach to enhance tight oil recovery is an efficient method (Sun et al., 2020). The efficiency of this enhanced oil recovery method is governed primarily by the properties of the rock formation (Ghanbari, 2015; Javaheri et al., 2018) and the characteristics of the injected fluids (Nowrouzi et al., 2020; Sun et al., 2020).

Researchers mainly focus on the influences of rock properties, including pore size, wettability, clay content, and other factors. In the spontaneous imbibition process, lower pore size can gain higher imbibition efficiency and production rate (Dou et al., 2021), indicating that the spontaneous imbibition predominantly affects the micropores. The reservoir ranging from 1 to 10 μm constitute the most important part for the imbibition process (Xiong et al., 2025), which can be attributed to the capillary pressure inversely proportional to the size of the pore and throat. Clay content impacts the imbibition efficiency mainly through mineral-water reactions (Yang et al., 2016). The clay

* Corresponding author.
E-mail address: shawnzhou326@126.com (X. Zhou).
Peer review under the responsibility of China University of Petroleum (Beijing).

https://doi.org/10.1016/j.petsci.2026.02.022
1995-8226/© 2026 The Authors. Publishing services by Elsevier B.V. on behalf of KeAi Communications Co. Ltd. This is an open access article under the CC BY license (http://creativecommons.org/licenses/by/4.0/).

minerals tend to expend in the water injection process, results in negative effects on the imbibition process, when clay content is higher than 40% (Xiong et al., 2025). Comparing the spontaneous imbibition rate in Fort Simpson, Muskwa and Otter Park shale formation, higher imbibition rate was observed in Fort Simpson shale, attributed to its higher clay content and consequent boosted water adsorption capacity (Dehghanpour et al., 2013; Ghanbari, 2015; Mehana et al., 2018). The ironic compositions of the formation water present complex influences on the spontaneous imbibition process. Some studies indicate that divalent ions in the brine (high salinity water) are benefit to the spontaneous imbibition, because the divalent ions in the water increase the wettability alteration strength, and thus higher oil recovery was obtained (Ghandi et al., 2019; Mehana et al., 2018). However, other researches demonstrate that salinity decrease the volume of imbibed water, due to salt restrain the diffuse electric double layer in the rock (Cai et al., 2020; Yan et al., 2025), leading to low imbibition efficiency.

Under different imbibition conditions, studies indicate that higher imbibition efficiency was obtained in the reservoir pressure and temperature with shorter equilibrium time compared to that under the standard laboratory conditions (Xiong et al., 2025). Higher reservoir temperature relates to higher imbibition efficiency, because the oil viscosity and interfacial tension (IFT) between oil and water phase can be reduced under higher temperature, as documented in studies of temperature effects on heavy-oil in fractured reservoirs. Pressure effects on the imbibition process have been investigated via comparative experiments at atmospheric pressure and 20 MPa using different chemical agents, the results show that the oil mainly produced from the smaller to medium-sized pores regardless of the effect of pressure (Chen et al., 2023). Anion–nonionic surfactant solution was used under different pressures, a recovery factor of 34.65% was gained under atmosphere pressure and 38.12% was achieved under the reservoir pressure (20 MPa) (Chen et al., 2023), confirming that the reservoir pressure increased the imbibition efficiency moderately. Notably, when the PAM slick water was employed in the imbibition process, oil recovery factor boosted from 26.31% to 41.55%, attributed to the smaller molecular of PAM slick improved the sweep efficiency in the fractures. Core geometry influences the production performance of the spontaneous imbibition process significantly. With cylindrical shape cores gained the highest imbibition rate, and an inverse influence on the imbibition rate was investigated from the characteristic of length. While a positive relationship was obtained for the exposed core surface and imbibition rate (Yildiz et al., 2006). Furthermore, studies on confining pressure reveal that ultimate oil recovery factor proportional to the confining pressure and higher than those without confining pressure (Jiang et al., 2018).

The performances of the imbibition process vary significantly with different injection fluids. Commonly used fluids are formation water, surfactant solution, etc. When formation water is employed, the main mechanism involves capillary force within throat and pore. That is because in the water-wet reservoir, the main driving force in the imbibition process is capillary force (Hu et al., 2020). The wetting phase invaded into the reservoir by sticking on the surface of the matrix, and displaced the non-wet phase (oil) out of the pore and throat (Xie et al., 2024). For the surfactant solution injection, the mechanisms for enhancing imbibition efficiency are capillary force, IFT reduction, emulsion of the oil, wettability alteration, etc. (Hu et al., 2020; Li et al., 2022; Santanna et al., 2014; Xie et al., 2024). When a surfactant solution is introduced into the reservoir, surfactant molecules orient at oil-water interfaces with hydrophilic groups adsorbed into water and hydrophobic group adsorbed into crude oil, leading to significantly IFT decreasing. The primary mechanisms for surfactant to reduce the IFT reduction lies in the adsorption of the injected surfactant solution on the rock surface, which minimizes the Gibbs free energy (Bahraminejad et al., 2019, 2022; Yekeen et al., 2019). Typically, an optimal surfactant concentration can be determined by comparing the IFT values. The amphiphilic nature of the surfactant enables formation of emulsion (oil in water), decreasing the oil viscosity and improving the oil mobility, so that enhancing oil recovery factor (Liu et al., 2024). Ion-pair is formed between surfactant and carboxylate in the oil (Standnes and Austad, 2000), the ion-pair dissolved into the oil phase, results in wettability alteration on the surface of rock (Kathel and Mohanty, 2013). Thereby enhancing the capillary force in the reservoir, and higher amount of water invasion into the pore space (Ghandi et al., 2019). In total, surfactant solution improves the wettability and reduces the IFT (Xu et al., 2025), resulting in higher imbibition efficiency. Furthermore, study demonstrates a positive correlation was investigated between the imbibition efficiency and the chemical solution concentration (Zhigarev et al., 2025). Nuclear Magnetic Resonance (NMR) technology has been extensively applied to clarify the distribution of pore size, by using T_2 spectra of the tight core (Liu et al., 2025; Lv et al., 2025; Zhang et al., 2022b). Because of the inverse relationship between capillary pressure and pore-throat size, the highest contribution of the oil recovery comes from nanopores (Cheng et al., 2019). Similar results are gained in the dynamic imbibition process, the oil recovery factor was obtained as highest in nanopores (3.0 nm to 1.7 μm), and lowest in micropores (1.7 μm to 8.5 μm) (Dai et al., 2019). Dynamic imbibition process indicates the highest imbibition efficiency occurred in the macropore (>32 μm), whereas in the spontaneous imbibition process the micropores (<3.2 μm) gained the highest imbibition efficiency (Dou et al., 2021). The T_2 spectra in the NMR experiments shows that the highest efficiency occurs in the pores ranges from 1 to 10 μm, while minimal recovery was investigated in the pores ranges from 0.1 to 0.5 μm (Xiong et al., 2025). From previous studies using NMR, the imbibition performance in pores and throats with the same range are different, mainly because the properties of the core and the fluids employed into the core. The imbibition efficiency and contribution for each pore type in the whole production process are rarely considered. So that to determine the imbibition performance, new experimental studies should be conducted.

The application of various surfactants in tight conglomerate and tight oil reservoirs has been shown to significantly enhance the oil recovery factor, mainly because of the IFT reduction and strong water-wet rock surface (Hu et al., 2020; Li et al., 2022; Santanna et al., 2014; Xie et al., 2024). With surfactant solution injection, the imbibition efficiency increased up to 61%, which is almost three times of that in water phase (Xiao et al., 2022). Different surfactants alone can raise the imbibition efficiency from 8.1% to 20%–30% in tight oil cores, while synergistic surfactants combinations have achieved efficiencies as high as 70.6% (Liu et al., 2023), and positive relationship is investigated between the imbibition efficiency and permeability. The present of artificial fractures, a key feature of reservoir stimulation, further amplifies this influence. Surfactant solution in fractured cores can enhance imbibition efficiency by approximately 50% compared to the cores without fractures, where about twofold was investigated (Yang et al., 2023a). In the Eagle Ford and Wolfcamp shale reservoirs, the imbibition efficiency for water phase is around 4%. But with surfactant solution (with a concentration of 0.2 vol%) application, the imbibition efficiency can boost up to 35% (Saputra et al., 2019). Even greater enhancement (up to 38.7%) has been achieved by combining surfactants (sodium lauryl ether sulfate) with nano-fluids such as SiO_2 (with a concentration of 0.05 wt%), compared to 10.75% for deionized water (Zhang et al., 2022a).

To investigate the influence of permeability and surfactant solution in imbibition process, experimental studies on pore-throat distribution, contact angle, IFT and lower limits of pore and throat size specification were implemented. The pore-throat distribution with different permeabilities were determined using the mercury intrusion apparatus. Pore size and throat diameter are measured ranges from 0.61 nm to 70.58 μm for the targeted cores, and four pore classes were defined. The contact angle for the core with water and surfactant solution decreased from 48.36° to 23.75°. Compared with the formation water injection, surfactant solution injection decreased the IFT from 23.92 to 9.69 mN/m. The lower limits of pore and throat size specification affected by the permeability and surfactant solution were determined using the NMR device. The results indicated that the lower limits of pore and throat size specification significantly decreased from water phase to surfactant solution phase, meaning that the utilization of the pore and throat were extremely extended. The findings in this study can be applied to guide the EOR processes applied in the tight conglomerate oil reservoirs.

2. Experimental study

2.1. Materials

Systematical study was carried out to investigate the performances of spontaneous imbibition process applied in tight conglomerate oil reservoir, four cores with varying permeability ranges were employed. A representative core was selected to establish the transformation coefficient between pore-throat size and the T_2 spectra in the NMR experiments. The oil sample and cores were both collected from western part of China (Xinjiang Oilfield). The components of the oil are listed in Table 1, the viscosity and density of the studied tight oil under the atmosphere condition are 2.15 mPa·s and 0.7562 g/cm^3, respectively. Cores properties are listed in Table 2, the permeability of the core for the imbibition tests ranges from 1.25 to 4.43 mD, and the porosity ranges from 6.59% to 12.90%. The relationship between permeability and porosity is investigated as not strictly positive correlation in the tight conglomerate formation (Yang et al., 2023b). The formation water (with a salinity of 13786.08 ppm) was collected from the same reservoir, the ion compositions are listed in Table 3. The surfactant solution with different concentrations (ranges from 0.05% to 0.20%) were employed to determine the imbibition efficiency in various cores. To avoid negative influence of the water phase in T_2 spectra measurement using NMR, 50 g/L $MnCl_2$ solution was employed to block the signal of hydrogen nucleus in the water phase (Ren et al., 2023; Xiao et al., 2021).

Table 1
Compositional analysis of the targeted tight oil sample.

Carbon No.	Mole fraction, mol%	Carbon No.	Mole fraction, mol%
C_6	0.04	C_{19}	4.03
C_7	2.18	C_{20}	2.71
C_8	4.70	C_{21}	2.40
C_9	8.22	C_{22}	2.38
C_{10}	8.14	C_{23}	2.35
C_{11}	5.84	C_{24}	2.04
C_{12}	6.66	C_{25}	1.98
C_{13}	8.24	C_{26}	1.55
C_{14}	5.24	C_{27}	1.17
C_{15}	7.83	C_{28}	0.88
C_{16}	3.58	C_{29}	0.69
C_{17}	9.00	C_{30+}	2.22
C_{18}	5.93	Sum	100.00

Table 2
Properties of the targeted tight conglomerate core sample.

Core number	Experiment	Length, cm	Diameter, cm	Porosity, %	Permeability, mD
#1	Mercury intrusion	5.22	2.51	14.80	0.22
#2	Spontaneous imbibition	4.26	2.47	7.12	4.43
#3		5.31	2.48	6.59	2.02
#4		4.41	2.45	12.62	1.89
#5		5.31	2.47	12.90	1.25

Table 3
Salinity and ion compositions of the studied formation water.

Ion composition and concentration, mg/L							pH	Salinity,
CO_3^{2-}	HCO_3^-	CL^-	SO_4^{2-}	Ca^{2+}	Mg^{2+}	Na^++K^+		ppm
49.31	211.65	8390.29	153.21	1621.82	394.96	3006.73	6.79	13786.08

2.2. Experimental setup

This study employed an integrated experimental approach utilizing four types of instruments including contact angle/IFT measurement device, mercury intrusion apparatus, spontaneous imbibition cell, and NMR device. The set-up of the experiments is shown in Fig. 1. An optical Contact Angle Measuring device (Theta Flex) was applied to measure the contact angles, using the liquid (formation water and surfactant solution) drop on the surface of core. The pore size and capillary pressure of the representative core could be determined using mercury intrusion apparatus (AutoPore V), results of the pore size will be analyzed with T_2 spectra to determine the transformation coefficient, which is used to transfer the relaxation time to pore size distribution. The production performance of the spontaneous imbibition applied in different cores with varying injection media (formation water and varying surfactant solutions) was carried out using the spontaneous imbibition cell. To determine the production performance in different certain pore-throat sizes, the NMR (MacroMR12-150H-I) was applied to measure the T_2 spectra of the cores. The relaxation signals of hydrogen in fluids can be determined by the NMR device (Ren et al., 2023; Xiao et al., 2021), so that the characterization of the pore-throat distribution can be implemented using the formation water saturated core.

2.3. Experimental procedure

In order to characterize imbibition behavior in the targeted reservoir, four complementary experiments were carried out. The detailed experimental procedures are indicated below.

(1) Wettability analysis of the surfactant solutions with varying concentrations was conducted using an optical Contact Angle Measuring device. Core samples were sectioned into small pieces with length of 1 cm, and the cross section was polished to ensure cleanliness and uniformity. Then contact angle was measured using the formation water and surfactant solution.
(2) The selected representative core sample was applied for the mercury intrusion test, the core was settled into the mercury intrusion device, and mercury was introduced into the core under a constant pressure. The results enabled quantitative determination of pore size distribution and capillary pressure in varying pore sizes.
(3) Formation water was firstly introduced into the core samples for T_2 spectra measurement. After that the cores were

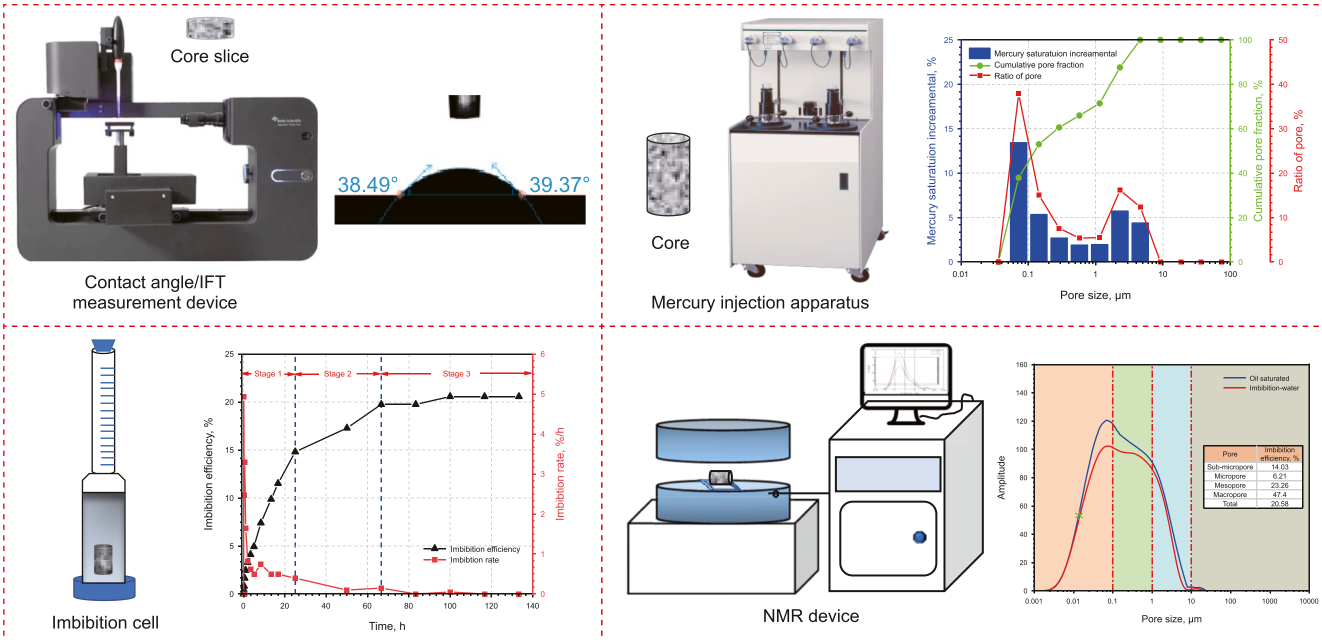

Fig. 1. Experiment set-up of the imbibition process applied in the tight conglomerate cores.

dried under 120 °C for at least 48 h to ensure no water exits in the cores. To eliminate the influences of the irreducible water, 50 g/L $MnCl_2$ solution was introduced to saturate the core, then oil saturation process was conducted in a core-holder under the reservoir condition (20.77 MPa, 59.1 °C). Totally, around 2 PV oil was introduced. The irreducible water saturation was established, and then T_2 spectra test using NMR was conducted to measure the oil distribution.

(4) The imbibition experiments were implemented by filling the imbibition cells formation water and surfactant solutions with the optimized concentration, respectively. The injected fluids were supplemented with $MnCl_2$, and ensure the concentration is 50 g/L. Each oil-saturated core was settled into the imbibition cell under ambient condition, then the imbibition system was sealed. The volume of produced oil was measured using the high accurate collection tube on the top of the cell, till no more oil produced in 12 h.

(5) Following the spontaneous imbibition experiment, the cores were subjected to T_2 spectra measurement using NMR. The residual oil distribution can be gained, then the imbibition efficiency in varying pores size were obtained by comparing the T_2 spectra before and after the imbibition process.

3. Results and discussion

Systematically study is carried out to investigate the pore-scale imbibition efficiency with different permeability cores through an integrated experimental approach. The concentration of the surfactant solution was optimized by the wettability measurement. The mercury intrusion process was implemented to clarify pore and throat distribution. Then spontaneous imbibition experiments were implemented in tight conglomerate cores with various permeabilities, to characterize the imbibition process. Furthermore, the oil distribution was investigated using NMR to determine the oil recovery factors and contributions in varying pores.

3.1. *Wettability and IFT measurement*

Once surfactant solution was employed into the targeted reservoir, it would affect the wettability of the formation rock (Hu et al., 2022; Lv et al., 2025), leading to IFT reduction and imbibition efficiency enhancement. An optical Contact Angle Measuring device was applied to measure the wettability of the core, the results of the measurement was indicated in Fig. 2. The measurement reveals that an initial contact angle of 48.36° with formation water, confirming that the targeted reservoir is water-wet characteristics formation. Surfactant solution application demonstrably decreased the IFT by sticking on surface of the rock and increasing the interfacial layer thickness, and thus extending the water film on the rock, results in contact angle decreasing (Ma et al., 2022). With the targeted tight conglomerate cores, the contact angle decreased with surfactant concentration increasing. The progressive contact angle reduction indicates that the wettability of the formation altered from water-wet to strong water-wet by introducing surfactant solution (Bin Dahbag et al., 2015).

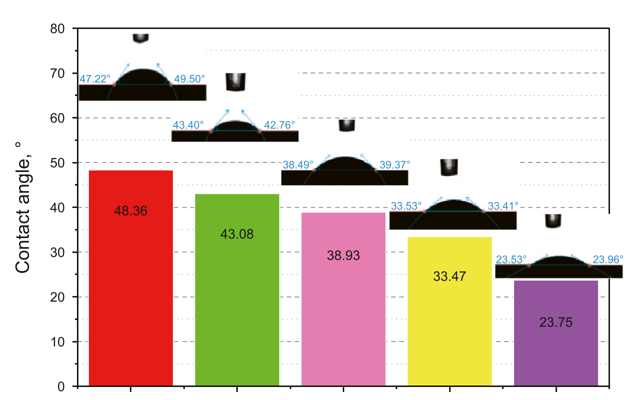

Fig. 2. Contact angles measurements for varying concentrations of surfactant solution (Note: SS-surfactant solution).

The IFT of the surfactant solution-oil systems were measured as presented in Fig. 3. For the formation water-oil system, the IFT was measured as 23.92 mN/m. Once surfactant solutions were employed into the formation, the adsorption process occurred on rock surface, the interfacial energy between fluid and rock was significantly decreased (Zhang et al., 2022a), leading to lower IFT was investigated. With addition of 0.05% surfactant solution, the IFT lowered remarkably to 11.93 mN/m. With increasing concentration, the IFT decreased, that is mainly because the higher concentration, the higher thickness of interfacial coverage of surfactant molecular on rock surface, and thus lower IFT (Ma et al., 2022). However, this relationship exhibits asymptotic characteristics as interfacial coverage reaches up to maximum on the rock surface, because the limitation of surfactant molecular stacking on the rock (Ma et al., 2022). For the surfactant concentration optimization, it mainly based on the type of the surfactant solution. Literature reported various optimum values, 0.10% was optimized for achieving the lowest IFT (Dai et al., 2019), 0.10 wt% for anionic surfactant solution yielding an oil recovery factor of 68% (Kathel and Mohanty, 2013), and 0.15% was employed for a SDBS surfactant because of the highest oil recovery (Yang et al., 2023). In this research, the concentration of the surfactant was optimized as 0.20%, mainly because of the lowest contact angle and IFT. A consistent trend was investigated, where both IFT and contact angle decrease with increasing surfactant concentration, up to around 0.30 wt%. That is mainly attributed to the fact that the critical micelle concentrations (CMC) of the surfactants were less than 0.30 wt% (Bahraminejad et al., 2021; Cao et al., 2022; Manshad et al., 2024).

3.2. Mercury intrusion experiment

To determine the size distribution of pore and throat in the cores, mercury intrusion experiment was implemented using a representative core in the targeted reservoir. The capillary pressure plot reveals the pore structure with the intrusion phase injection, as indicated in Fig. 4. Initially, the capillary pressure increased quickly with mercury intrusion, that is mainly due to mercury is the non-wetting phase, so the capillary pressure presents as entry resistance. In the first intrusion stage (mercury saturation 0%), the injected mercury firstly invaded into the relatively large pores, and the capillary pressure reached up to around 0.16 MPa at a characteristic pore-throat diameter of 4.594 μm. The

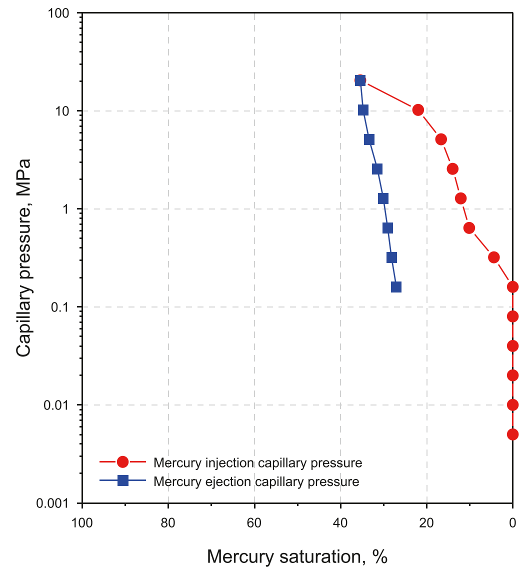

Fig. 4. Capillary pressure measured in mercury injection/ejection process.

second stage (mercury saturation ranges from 0 to 10%) exhibited a reduced incremental ratio of the capillary pressure, reflecting the injected mercury mainly occupied the large pores, and the capillary pressure was mainly affected by the heterogeneity of the core. The capillary pressure reached to 0.64 MPa with pore size decreased to 1.148 μm. In the third stage (mercury saturation higher than 10%), mercury invaded into relatively small pores and throats, so that the capillary pressure increased remarkably. When the lowest size of pore and throat was invaded, the capillary pressure reached up to 20.48 MPa with a mercury saturation of 35.41%.

Mercury intrusion experiments revealed the size of the pore and throat, ranging from 0.036 to 4.594 μm, as indicated in Fig. 5. The mercury saturation incremental indicates the fractions of pore volumes with different sizes. For the targeted reservoir, the size of main pore ranges from 0.072 to 0.144 μm and 2.297 to 4.594 μm, the fractions of those pores are 52.99% and 28.55%, respectively. Small pores were investigated as the most part of the pores in the tight conglomerate cores, with a maximum radius of 2.07 μm for the connected pores and an average pore radius of 0.39 μm. The capillary pressure of the medium value mercury saturation is 5.12 MPa, and the sorting coefficient, variation coefficient and pore to throat volume ratio are 1.90, 0.15 and 3.24, respectively.

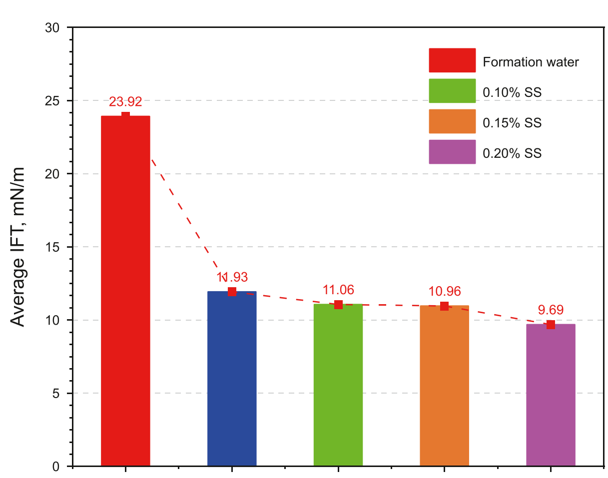

Fig. 3. IFT measurements for surfactant solution with varying concentrations (Note: SS-surfactant solution).

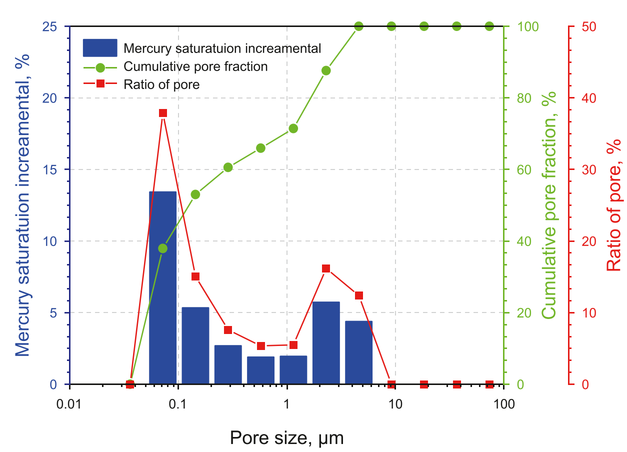

Fig. 5. The experimental results of the mercury intrusion experiment.

Based on the established NMR theory for applying in the oil recovery (Jiang et al., 2023; Xu et al., 2022), NMR was used to determine the oil saturation in varying pores, reflecting the pore and throat distribution. The fundamental principle of T_2 spectra measurement in the NMR test is that the interaction between hydrogen nucleus in the fluid and the magnetic field (Tan et al., 2015). And a proportional relation was investigated between the amount of hydrogen nucleus and amplitude of the T_2 spectra (Ren et al., 2023), this physical relationship enables pore and throat characterization using fluids injected into the core. The comparative analysis of the T_2 spectra before and after the imbibition process provides quantitative assessment of oil distribution in varying pore and throat.

According to the fundamental principle of T_2 spectra, the T_2 is determined by Eqs. (1)–(3) (Jiang et al., 2023; Tan et al., 2015; Xiao et al., 2021; Xu et al., 2022).

$$\frac{1}{T_2}=\frac{1}{T_{2B}}+\frac{1}{T_{2s}}+\frac{1}{T_{2D}} \tag{1}$$

$$\frac{1}{T_{2s}}=\rho_2\left(\frac{S}{V}\right)_{\text{Pore}} \tag{2}$$

$$\frac{1}{T_{2D}}=\frac{D(\gamma G t_E)^2}{12} \tag{3}$$

where T_2 is the relaxation time in the NMR test, ms. T_{2B} is the bulk relaxation, which relates to the properties of the fluids, ms. ρ_2 is the surface relativity, μm/ms. S is the surface area of the pore, μm^2. V is the volume of the pore, μm^3. D is the self-diffusion coefficient of the fluids, m^2/s. γ is the gyromagnetic ratio of hydrogen nucleus, rad/(sT). G is the internal magnetic field gradient, T/m. t_E is the echo time of the apparatus, s.

Usually, T_{2B} is ignored mainly because in a uniform magnetic and water-wettable core with brine saturated, T_{2B} is relatively higher than 3000 ms (Xiao et al., 2016, 2021), which is much higher than T_2. T_{2D} can be disregarded due to it determined by the magnetic field and t_E is much small in the core. Therefore, T_2 is proportional to T_{2S}, which relate to pore size (surface and volume) in the NMR measurements.

In order to convert relaxation time in T_2 spectra to pore-throat size distribution, a simplified equation was used, as indicated in Eq. (4). This approach enables precise determination of oil distribution in varying pores, the contribution can be obtained for each certain pore.

$$r=C\times T_2 \tag{4}$$

where r is the diameter of the pore and throat, μm; T_2 is the relaxation time in the T_2 spectra, ms; C is the transformation coefficient from T_2 to r, μm/ms.

Once the targeted core was saturated with oil using both vacuum pump and core-holder (Zhou et al., 2022), the NMR test was conducted, and the T_2 spectra was shown in Fig. 6. The relaxation time mainly ranges from 0.2 to 130 ms, the pore size ranges from 0.072 to 9.188 μm. According to the approach for clarifying the transformation coefficient applied in the tight oil reservoirs (Xiao et al., 2021), the maximum pore size was calibrated against the highest relaxation time in the T_2 spectra to achieve optimal alignment between plots of the ratio of pores and relaxation time. The transformation coefficient was obtained as 0.0405 μm/ms, enabling accurate conversion of relaxation time to pore size distribution. Because the cores were collected from the same well, so that the transformation coefficient calculated in core #1 can be applied in other cores, as indicated in previous studies (Huang et al., 2025; Xiao et al., 2021).

Pore distributions across varying cores were characterized using NMR, as indicted in Fig. 7. To investigate the production performance in different cores, pores and throats were categorized into four classes according to the diameter of each pore. The four classes are sub-micropore (<0.1 μm), micropore (0.1–1 μm), mesopore (1–10 μm) and macropore (>10 μm), respectively. Due to proportional relationship between the amplitude in T_2 spectra and the amount of hydrogen nucleus, the amplitude indicates the volume of the pores in the core. Comparative analysis reveals that with a higher porosity (cores #4 and #5), the amplitude is much higher than that of the cores with a lower porosity (cores #2 and #3), indicating greater total volumes of porous for oil saturation in cores with higher porosity.

The fraction of different pore classes within the core was quantified via integration of T_2 spectra. The fraction for each certain pore class can be determined using its segmental integral area divided by the total integral area of the T_2 spectra. The fractions of varying pore classes for each core can be seen in Fig. 8. The fractions of the mesopore are much higher in the targeted cores, which is higher than 66% for each core, and the highest reaches up to 76.52% for core #2. 10%–20% was investigated for the micropores, meaning that the main pores in the targeted cores are mesopore and micropore.

Unlike conventional reservoirs, the relationship between porosity and permeability in conglomerate formation deviates

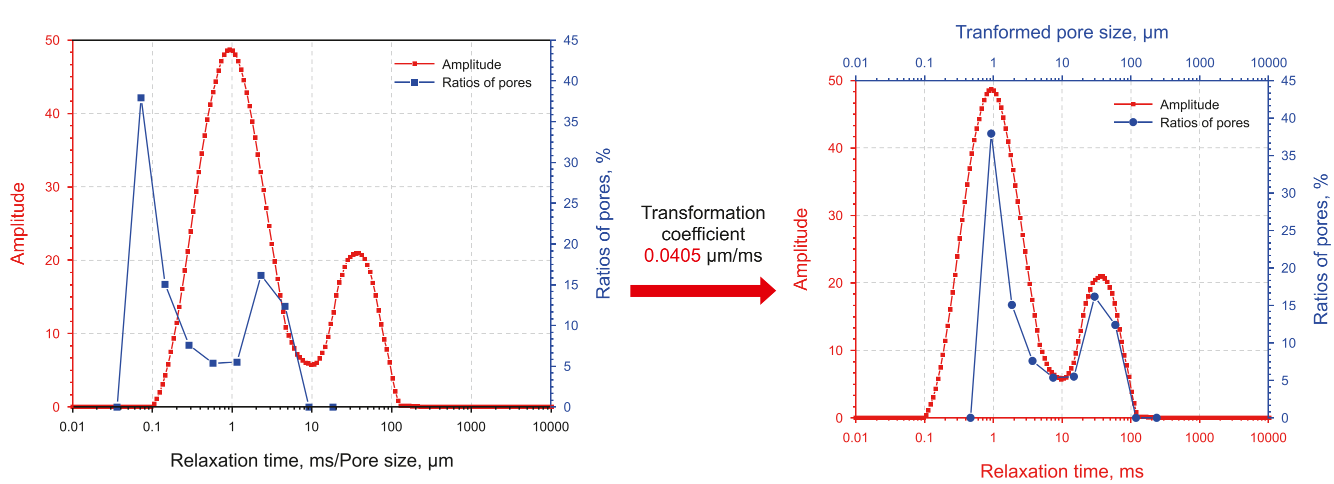

Fig. 6. Plots for determining transformation coefficient of T_2 spectra and pore-throat size distribution.

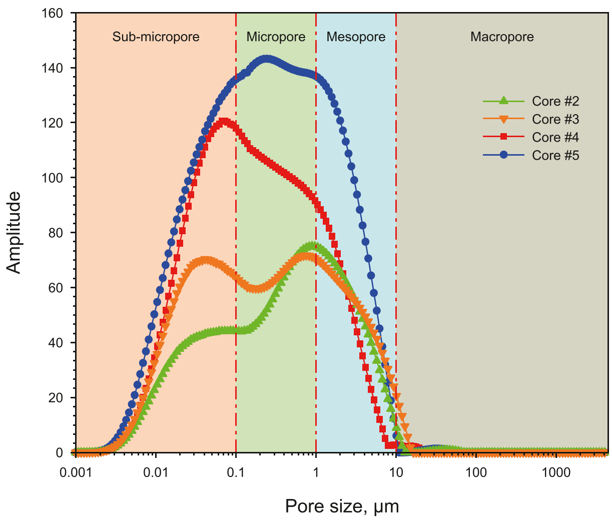

Fig. 7. Pore size distribution of different cores via NMR test.

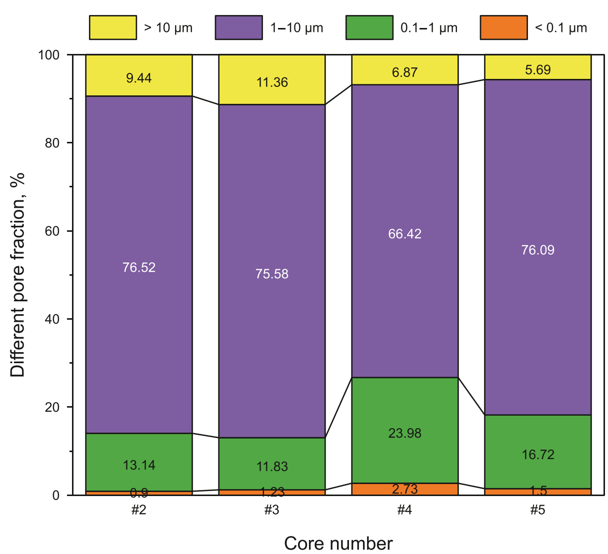

Fig. 8. Fractions of different pores in the targeted formation cores.

from a liner trend, as illustrated in Fig. 9. The results demonstrate a characteristic pattern where porosity initially decreases with decreasing permeability, then exhibits an increasing trend, reflecting the absence of consistent linear between these parameters in conglomerate cores, these findings similar to previous studies (Jiang et al., 2025; Liu et al., 2025; Tian et al., 2022). This anomaly primarily stems from the significant size of gravel within the core, which creates strong heterogeneity (Liu et al., 2025). Furthermore, the presence of microfractures in the cores enhances the connections among the pores, their diameter and length vary considerably across different cores. The nature microfractures act as high-permeability channels, leading to preferential paths for high-rate fluid migration and relative higher permeability with low porosity (Zhang et al., 2025). The combined influences of heterogeneous gravel distribution and variable microfractures ultimately disrupt the conventional porosity-permeability relationship observed in homogeneous reservoirs. Consequently, established equations for predicting the relationship between permeability and porosity cannot be applied in the conglomerate cores. 3-D pore structure model and ball-stick model of the

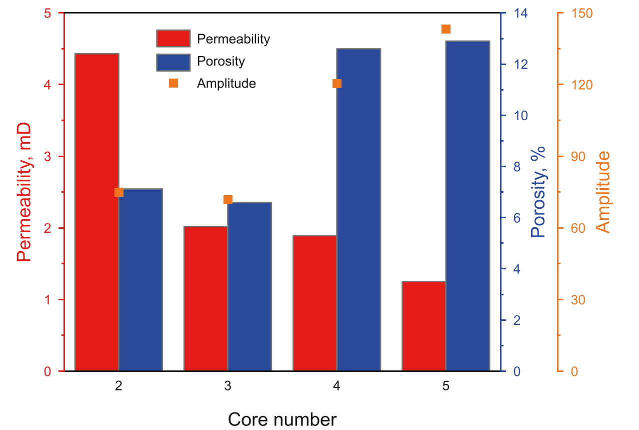

Fig. 9. Relationship between permeability, porosity and amplitude in the tight conglomerate reservoir.

conglomerate core indicate that many pores within the conglomerate core are isolated or weakly connected, thus positive relationship between porosity and permeability is not gained in conglomerate cores (Zhang et al., 2025). Therefore, non-liner relationship is gained between porosity and permeability of the studied tight conglomerate cores. However, a positive correlation was obtained between the porosity and the amplitude within the NMR measurement. That is because porosity of the core shows the total volume of the pore and throat, and the amplitude indicates the amount of hydrogen nucleus in the core. The higher volume of the pore and throat, higher amount of hydrogen nucleus can be obtained.

3.3. Characteristics of core scale spontaneous imbibition

Spontaneous imbibition experiments were implemented using cores with various permeability in formation water and 0.20% surfactant solution, respectively. Taking the experiment with core #4 in formation water as an example, the imbibition performance was divided into three stages, as indicated in Fig. 10. Stage one is the rapid imbibition stage. Formation water invaded into the cores via capillary pressure, oil in the relatively larger pores (mesopore and macropore) was displaced. Because the oil volume in these relative larger pores is higher, the imbibition efficiency increased sharply. The imbibition efficiency in this stage reached up to 15%, and the imbibition rate was much higher than those in other stages, at 4.99 %/h. Stage two is the moderate imbibition stage. After the oil in the relatively large pore (mesopore and micropore) was displaced, the introduced fluids began to invade into the small-size pores, and the imbibition rate decreased to 0.15–0.40 %/h. Stage three is the equilibrium imbibition stage. In this stage, small pores (sub-micropore) were displaced by the injected fluids, and the oil imbibition efficiency stabilized. This is because oil in small pores and remaining oil in large to medium pores were tiny, causing the imbibition process to stabilize.

The pore-scale characteristics of the imbibition process using formation water are investigated in Fig. 11. With the introduction of formation water, oil in the four classes of pores were produced. The highest imbibition efficiency is observed in macropore, reaching 47.40%, which is primarily attributed to their lower capillary pressure, facilitating easier oil displacement by the invading formation water. In contract, capillary pressure increases as pore size decrease, so that the imbibition efficiency in the sub-micropores is higher than that in the micropores. The maximum NMR amplitude decreased from 120 a.u. to 102 a.u. indicates a

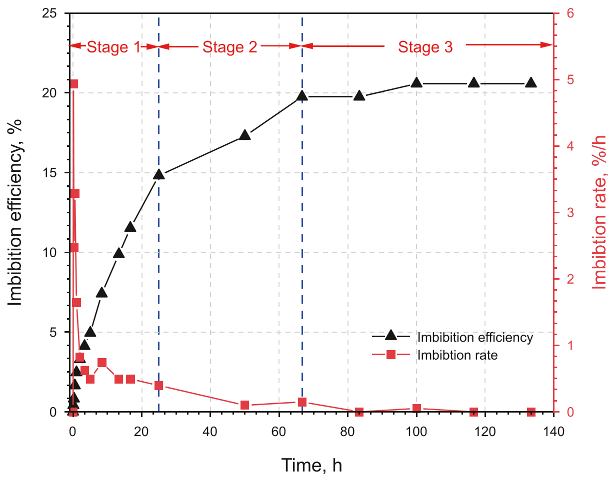

Fig. 10. The imbibition performance plots of tight conglomerate core #4 using formation water.

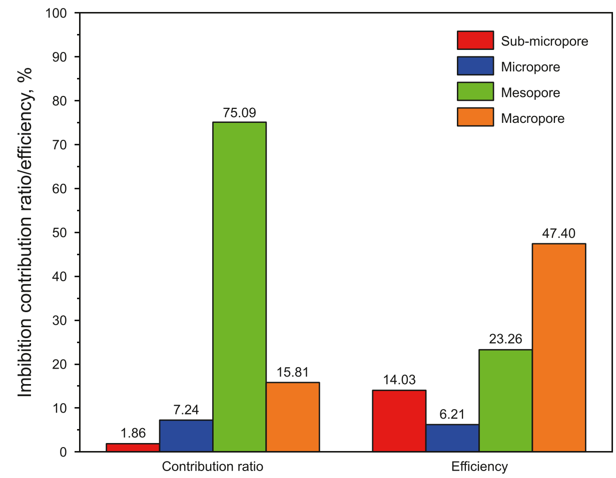

Fig. 12. Imbibition contribution and efficiency of formation water in core #4.

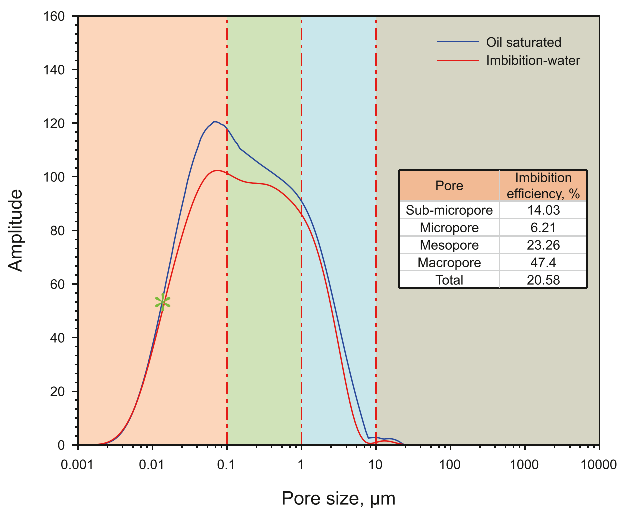

Fig. 11. T_2 spectra for the imbibition process using formation water in core #4.

reduction of the amount of hydrogen nucleus within the oil phase after formation water imbibition, corresponding to a total imbibition efficiency of 20.58%. The lower limit of pore size was defined as the point at which the spectra begin to diverge (marked by a star in the figure) between the two T_2 spectra (initial oil saturation and formation water imbibition). The lower limit of pore throat size was calculated as 0.013 μm for core #4, meaning that oil in the pore and throat lower than 0.013 μm cannot be produced using formation water imbibition process in this core.

In order to evaluate production performances across varying pores in core #4, the imbibition contribution ratio and imbibition efficiency were analyzed, as shown in Fig. 12. The contribution ratio is defined as volume of oil produced in varying pores divided by the total volume of oil produced from the core. The imbibition efficiency for each class pore is defined as the volume of oil produced from it divided by the initial oil volume saturated within it, the volumes were quantified by integrating the areas in the T_2 spectra. The highest imbibition efficiency was observed in macropore at 47.40%, followed by mesopore at 23.26%. Despite the high capillary pressure in sub-micropore, which led to an imbibition efficiency up to 14.03%, the contribution ratio was minimal to 1.86%. That is because the total pore volume of the sub-micropore is exceedingly small. Conversely, mesopores provided the dominant contribution to oil production with 75.09%, as they represent the primary pore system in this tight conglomerate reservoir. Although macropores exhibited the highest displacement efficiency, their limited total volume resulted in a lower overall contribution ratio of 15.81%.

3.4. Effect of injection media

With the optimized surfactant concentration of 0.20%, an imbibition process was implemented. Take core #2 as an example, the T_2 spectra for formation water and surfactant solution were both indicated in Fig. 13. The T_2 spectra after surfactant solution was significantly lower than that after formation water imbibition across in all pore classes. That indicates a greater oil recovery from all pore classes achieved by the surfactant solution. That is because of the diffusion of surfactant molecules to the water-oil, oil-matrix and water-matrix interfaces (Paria and Khilar, 2004; Wang et al., 2021), which remarkably decreased the IFT (Cao et al., 2022; Dai et al., 2019). In this study, the IFT reduced from 23.92 mN/m to 9.69 mN/m by the injection of surfactant solution with concentration of 0.20%, a phenomenon consistent with previous studies (Ding et al., 2024; Hou et al., 2022; Wang et al., 2023). This IFT reduction mechanism facilitates higher imbibition efficient, boosting the cumulative imbibition efficiency for core #2 from 16.31% to 27.62%.

The introduction of varying media enhanced imbibition efficiency across all four class pores, as indicated in Fig. 14. Compared to the imbibition performance of formation water, in the sub-micropores with pore size lower than 0.1 μm, the inherently high capillary pressure combined with the IFT reduction and wettability alteration induced by the surfactant solution, leading to a remarkable enhancement of imbibition efficiency from 20.15% to 31.92%. The imbibition efficiencies for the micropore, mesopore and macropore are 16.59%, 10.43% and 10.97%, respectively. However, the contribution ratio for sub-micropore and mesopore decreased, but those in the micropore and macropore increased. That discrepancy arises from the dual influences of the surfactant solution. On the one hand, with the benefit influences of capillary pressure, IFT reduction and wettability alteration, the injected surfactant solution can enhance the imbibition efficiency in different class pores. On the other hand, it can emulsify oil into the discreate droplets. If the diameter of the droplet is greater than the pore size, it stuck off narrower throat in the pore, thus the droplet

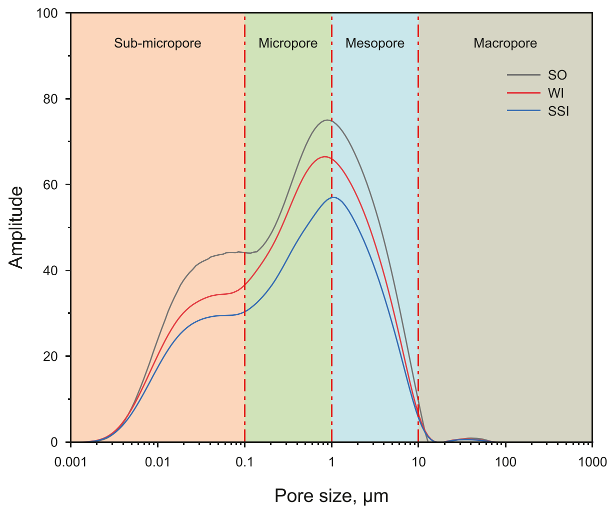

Fig. 13. The imbibition performances for different injection media applied in core #2 (Note: SO-saturated oil, WI-formation water imbibition, SSI- surfactant solution imbibition).

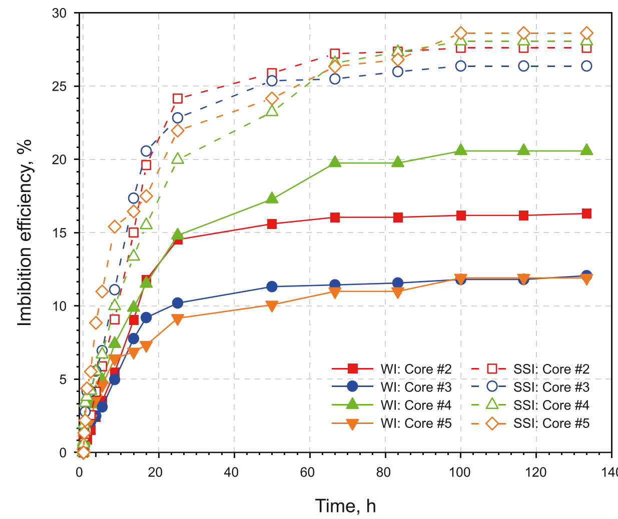

Fig. 15. Imbibition performance plots of formation water and surfactant solution applied in various cores.

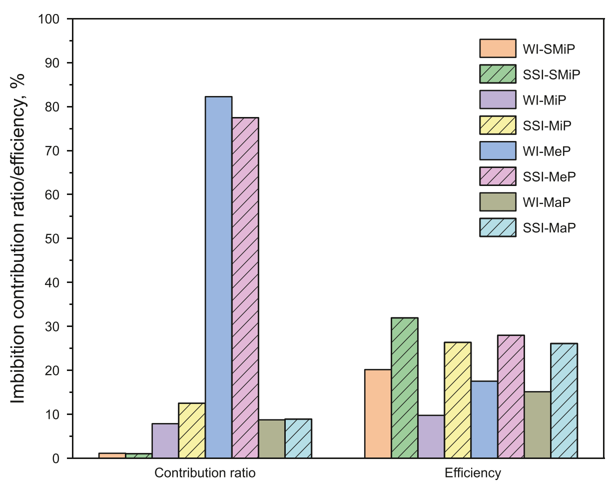

Fig. 14. Imbibition contribution ratio and efficiency of formation water applied in core #2 (Note: SMiP-Sub-micropore, MiP-micropore, MeP-mesopore, MaP-macropore).

presents as obstacles for enhancing oil production (Xu et al., 2025). The net influences of these competing mechanisms (enhanced imbibition efficiency, potential throat blockage) vary by pore class, leading to non-uniform changes in the contribution ratio.

The imbibition efficiency for different cores were indicated in Fig. 15. During formation water imbibition process, the imbibition efficiency ranged from 11.91% to 20.58%, with most of the oil production occurring rapidly within the first 25 h (stage 1). The rapid oil production is attributed to capillary-driven, when oil is displaced from smaller pores into larger flow pathway. However, the moveable oil volume accessible under capillary force alone is limited, causing the process to plateau rapidly. Due to the nonliner relationship between permeability and porosity in the tight conglomerate cores, different trends between imbibition efficiency and pore size were investigated (Liu et al., 2024). A phenomenon is investigated that, the imbibition efficiency does not uniformly increase with permeability across varying pore classes, the imbibition efficiency increases in the mesopore and macropore, while decreasing in the macropore, consistent with previous investigation (Liu et al., 2024; Wang et al., 2023), the imbibition efficiency is not liner relationship with permeability. The presence of microfractures, which increases the fluid-contact area and provide flow pathway (Wang et al., 2023), is a key effect to higher imbibition efficiency in some cores, overriding the influence of intrinsic permeability. In contrast, surfactant imbibition significantly enhanced oil recovery, with the imbibition efficiency reaching up to 28.63%. This improvement is primarily due to wettability alteration and IFT reduction, which synergistically enhance oil mobility and imbibition efficiency.

The imbibition process applied in tight conglomerate core is characterized by a dominant initial stage (stage 1), where the imbibition rate is highest, as indicated in Fig. 16. The imbibition rates are much higher in the beginning, for formation water and surfactant solution are 5.35 %/h and 8.33 %/h, respectively. The higher imbibition rate for surfactant solution is mainly because of a substantial reduction of IFT (Guo et al., 2020), which facilitates oil mobilization. However, the imbibition rate declined sharply after the first 2 h, falling to around 1 %/h for surfactant and 0.5 %/h for formation water, respectively. After about 17 h, the imbibition rate decreased remarkably, and oil recovery maintains stabilized, indicating that the spontaneous imbibition process has a limited effective range in these tight formations.

3.5. Effect of rock properties

The cores used in the imbibition process were collected from the same oil reservoir, primarily differ in permeability, permeability of the core ranges from 1.25 to 4.43 mD. The imbibition efficiency in various pores for each core could be investigated in Fig. 17. During formation water injection, lower permeability core (core #5) exhibited higher imbibition efficiency in submicropore and micropore. That is mainly because the stronger capillary pressure prevails in the relative narrower throat. However, for the macropore, much higher imbibition efficiency is investigated in lower permeability core, and the imbibition efficiency reaches up to 57.77%. This counterintuitive result is mainly because superior macropore connectivity in core #5, which minimized capillary trapping of oil droplets. In contrast, with higher-permeability, core #2 despites its overall permeability, has lower porosity, which likely indicates poorer macropore connectivity. This would lead to the trapping of mobilized oil droplets at constricting throats between macropores, thereby reducing

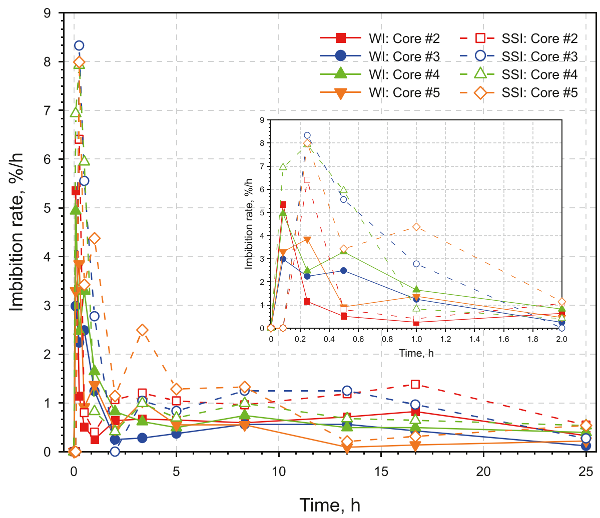

Fig. 16. Imbibition rate plots of formation water and surfactant solution applied in various cores.

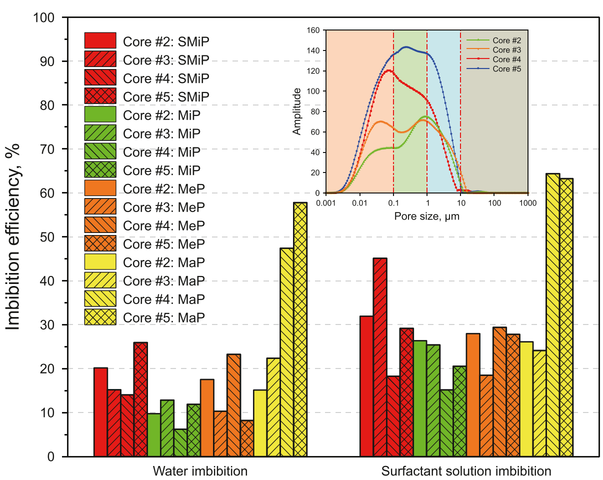

Fig. 17. Imbibition efficiency of formation water and surfactant solution in varying pores.

efficiency. Across all cores, micropores consistently showed the lowest imbibition efficiency. The pore size (0.1–1 μm) is likely comparable to the size of oil droplets, leading to frequent throat blockage and restricted flow, even with surfactant assistance. The highest imbibition efficiency occurred in the macropore, as these large pores and throats serve as main flow channels, facilitating higher imbibition efficiency. Oil phase in the lower pores would pass through the channels when it was flooded by the invaded liquid. With surfactant solution injection, the imbibition efficiency was increased significantly in all pores for the studied cores, demonstrating its effectiveness in improving overall oil recovery. Among the four pore types, the medium size pores exhibited the lowest imbibition efficiency. This investigation is consistent with previous research, which indicates pores size around 18.4 μm gained the lowest imbibition efficiency under various injection rates. This phenomenon can be attribute to the distinct roles of different pores classes. With micropores (ranges from 1.7 to 8.5 μm) act as primary conduits for oil flow, the oil saturation within the medium-size pores is predominantly governed by the interplay between capillary pressure and viscous force (Dai et al., 2019).

The contribution of varying pore classes to total oil recovery is compared in Fig. 18. Due to their dominant pore volume (ranging from 66.42% to 76.52%), mesopores constitute the primary part of produced oil, despite having moderate imbibition efficiencies of around 15% for formation water and 25% for surfactant solution, respectively. And high contribution ratios were observed for formation water and surfactant imbibition as around 65% and 70%, respectively. In contrast, although sub-micropores exhibit relatively high imbibition efficiency because of the stronger capillary pressures, their minuscule pore volume leads to the lowest imbibition contribution ratio, at merely 2%. Therefore, it can be concluded that mesopores serve as the main oil producing area in the studied tight conglomerate reservoir.

The imbibition performances for different cores under various injection media were shown in Fig. 19. With formation water and surfactant solution injection, imbibition occurred in all pore classes, leading to reduction in the T_2 spectra across all pores for each core, indicating the oil production across the entire pore structures. For cores #2 and #4, the T_2 spectra decreased uniformly with formation water and surfactant solution injected, indicating the pore and throat are relatively uniform. For cores #3 and #5 showed a pronounced T_2 spectra reduction in the sub-micropore and micropore with fluids injection. This implies high connectivity specifically within the smaller pore networks of these cores. In the mesopore for core #5, minimal change was investigated in T_2 spectra after formation water imbibition, with the spectrum remaining close to its initial oil-saturated state. This may because of poor connectivity or ineffective formation water displacement in the mesopores of this core.

Once the fluids were introduced into the tight conglomerate oil reservoir, imbibition process occurred, and oil in varying pores and throats were produced. With varying injection fluids, the lower limits of pore and throat size in the imbibition process are various, as listed in Table 4. During formation water injection process, the lower limits of pore and throat size for the studied cores ranges from 0.008 μm to 0.021 μm. Consequently, oil residing in pores smaller than 0.008 μm could not be produced and remained as residual oil in the core. In contrast, with surfactant solution injection, the lower limits of pore throat size reduced in all cores (ranges from 0.003 μm to 0.007 μm), thereby mobilizing a substantial volume of oil from the sub-micropores.

The cumulative imbibition efficiency for the studied cores with different permeability are summarized in Table 5. With formation

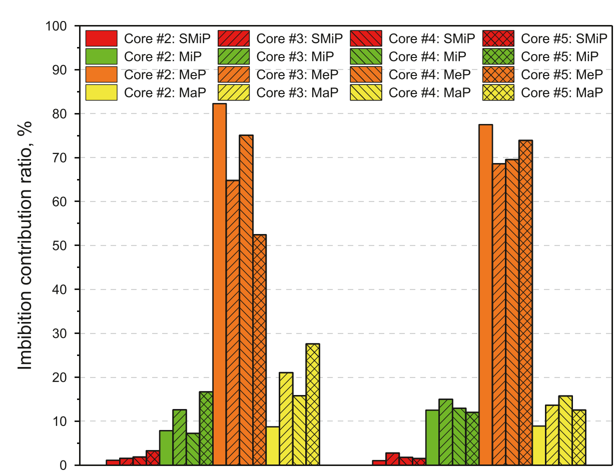

Fig. 18. Imbibition contribution ratio of formation water and surfactant solution in different pores.

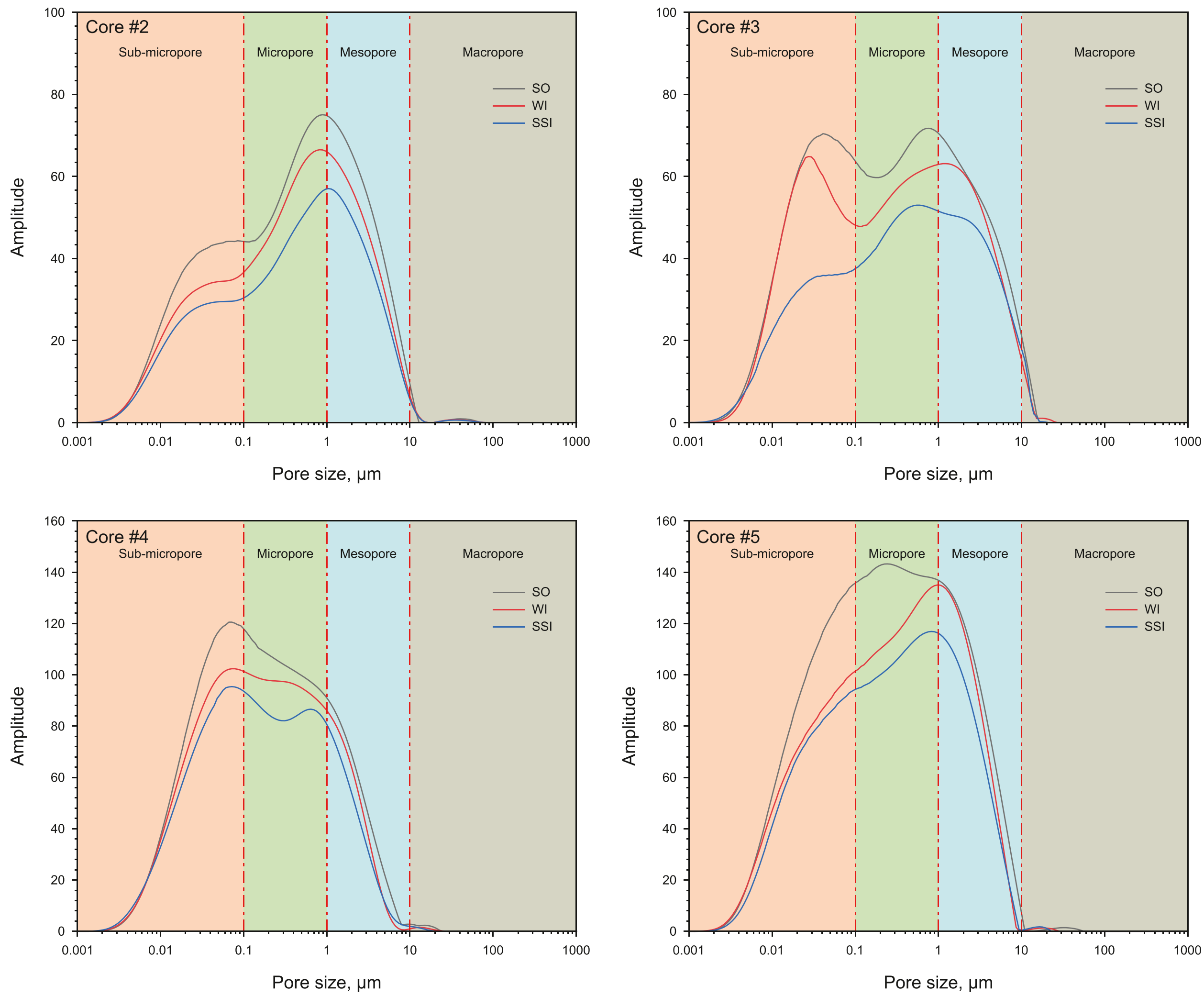

Fig. 19. T_2 spectra for various injection media applied in different cores.

Table 4
Lower limits of pore-throat size for each core with various injection media.

Core number	Lower limits of pore-throat size, μm	
	Formation water imbibition	Surfactant solution imbibition
#2	0.013	0.004
#3	0.021	0.005
#4	0.012	0.007
#5	0.008	0.003

Table 5
Imbibition efficiency for each core with various injection media.

Core number	Imbibition efficiency, %		Efficiency enhancement, %
	Formation water imbibition	Surfactant solution imbibition	
#2	16.31	27.62	11.31
#3	12.06	26.37	14.31
#4	20.58	28.07	7.49
#5	11.91	28.63	16.72

water injection, the imbibition efficiency ranged from 11.91% to 20.58%. With surfactant solution injection, the IFT of the water-oil phase decreased significantly and the water wettability of the matrix increased. The imbibition efficiency enhanced around 10% on average. The core #5 achieved the highest cumulative imbibition efficiency of 28.63%, which corresponds to an enhancement of 16.72%. This superior imbibition performance is because the injected surfactant solution extends the lower limits of pore throat size to as low as 0.003 μm. Therefore, imbibition is one key mechanism to improve oil production using fluids injection in the tight conglomerate oil reservoir. Based on the experimental study of imbibition under core scale, the imbibition process shows high potential for application at the reservoir scale. When a surfactant solution is injected into a reservoir, it preferentially flows through zones of relatively higher permeability, initiating an imbibition occurred along the flooding mechanism. And the main oil production was observed as in small to medium-sized pores (Chen et al., 2023). While the flooding front primarily influences medium to large pores, the surfactant, owing to its tiny molecular size, can penetrate from these lager throats into adjacent micropores and sub-micropores, thereby mobilizing the oil therein. As the volume of injected fluids increases, both flooding efficiency and the area of the injected fluids distribution expand substantially. Consequently, the reservoir volume influenced by the imbibition mechanism is significantly enlarged, leading to a remarkable enhancement in total oil production.

4. Conclusions

Four kinds of experiments were implemented to study the influences of core properties and surfactant solution influences on the imbibition process. From the experimental studies, four conclusions are drawn.

(1) For tight conglomerate reservoir, non-liner relationship is investigated between the permeability and porosity for varying cores, which is mainly due to the variable size distribution of gravel and micro-fractures. Pore system analysis reveals that mesopore contribute the main pore type, accounting for 66.42% to 76.52% of the total volume in the targeted reservoir.
(2) An inversely relationship between the surfactant solution concentration and both contact angle and IFT is gained. Compared with the formation water, with an optimal concentration of 0.20% surfactant solution, the contact angle decreases from 48.36° to 23.75°, and the IFT decreases from 23.92 mN/m to 9.69 mN/m.
(3) The highest imbibition contribution ratio is investigated in the mesopore for the targeted cores, indicating that the mesopores are main potential for oil production in the tight conglomerate oil reservoir. The imbibition contribution ratio for formation water ranges from 52.43% to 82.27%, and for surfactant solution ranges from 68.53% to 77.50%.
(4) Compared with formation water injection, the application of a surfactant solution with concentration of 0.20% in the tight conglomerate reservoir significantly reduced the lower limit of producible pore-throat size from 0.008–0.021 μm to 0.003–0.007 μm. And with surfactant solution injection, the imbibition efficiency is enhanced by around 10% than that for formation water injection.

CRediT authorship contribution statement

Xiang Zhou: Writing – original draft, Validation, Supervision, Methodology, Data curation. **Zhong-Wen Hu:** Validation, Methodology, Data curation. **Feng Wang:** Validation, Data curation. **Zhao-Wen Jiang:** Data curation. **Yu-Long Zhao:** Writing – review & editing, Investigation. **Tao Zhang:** Writing – review & editing. **Lie-Hui Zhang:** Writing – review & editing, Project administration. **Qi Jiang:** Writing – review & editing.

Declaration of competing interest

The authors declare that they have no known competing financial interests or personal relationships that could have appeared to influence the work reported in this paper.

Acknowledgments

The authors would like to acknowledge the financial support from the National Natural Science Foundation of China (No. 52374049), the Sichuan Science and Technology Program (No. 2026NSFSC0338), and the Oil & Gas Major Project (No. 2025ZD1407504).

References

Bahraminejad, H., Khaksar Manshad, A., Riazi, M., Ali, J.A., Sajadi, S.M., Keshavarz, A., 2019. CuO/TiO_2/PAM as a novel introduced hybrid agent for water—Oil interfacial tension and wettability optimization in chemical enhanced oil recovery. Energy Fuel. 33, 10547–10560. https://doi.org/10.1021/acs.energyfuels.9b02109.
Bahraminejad, H., Manshad, A.K., Keshavarz, A., 2021. Characterization, micellization, behavior, and performance of a novel surfactant derived from gundelia tournefortii plant during chemical enhanced oil recovery. Energy Fuel. 35, 1259–1272.
Bahraminejad, H., Manshad, A.K., Iglauer, S., Keshavarz, A., 2022. NEOR mechanisms and performance analysis in carbonate/sandstone rock coated microfluidic systems. Fuel 309, 122327. https://doi.org/10.1016/j.fuel.2021.122327.
Bin Dahbag, M., AlQuraishi, A., Benzagouta, M., 2015. Efficiency of ionic liquids for chemical enhanced oil recovery. J. Pet. Explor. Prod. Technol. 5, 353–361. https://doi.org/10.1007/s13202-014-0147-5.
Cai, J., Li, C., Song, K., Zou, S., Yang, Z., Shen, Y., Meng, Q., Liu, Y., 2020. The influence of salinity and mineral components on spontaneous imbibition in tight sandstone. Fuel 269, 117087. https://doi.org/10.1016/j.fuel.2020.117087.
Cao, B., Lu, X., Xie, K., Ding, H., Xiao, Z., Cao, W., Zhou, Y., He, X., Li, Y., Li, H., 2022. The pore-scale mechanisms of surfactant-assisted spontaneous and forced imbibition in water-wet tight oil reservoirs. J. Pet. Sci. Eng. 213, 110371. https://doi.org/10.1016/j.petrol.2022.110371.
Chen, Y., Wei, J., Hadavimoghaddam, F., Zhou, X., Ostadhassan, M., Zhao, X., Gayubov, A., Li, J., Wang, A., Yang, Y., Shi, X., 2023. Experimental study of oil recovery mechanisms during imbibition in tight sandstone with different fluid displacing agents under ambient and reservoir pressure. J. Pet. Sci. Eng. 220, 111181. https://doi.org/10.1016/j.petrol.2022.111181.
Cheng, Z., Ning, Z., Yu, X., Wang, Q., Zhang, W., 2019. New insights into spontaneous imbibition in tight oil sandstones with NMR. J. Pet. Sci. Eng. 179, 455–464. https://doi.org/10.1016/j.petrol.2019.04.084.
Dai, C., Cheng, R., Sun, X., Liu, Y., Zhou, H., Wu, Y., You, Q., Zhang, Y., Sun, Y., 2019. Oil migration in nanometer to micrometer sized pores of tight oil sandstone during dynamic surfactant imbibition with online NMR. Fuel 245, 544–553. https://doi.org/10.1016/j.fuel.2019.01.021.
Dehghanpour, H., Lan, Q., Saeed, Y., Fei, H., Qi, Z., 2013. Spontaneous imbibition of brine and oil in gas shales: effect of water adsorption and resulting microfractures. Energy Fuel. 27, 3039–3049. https://doi.org/10.1021/ef4002814.
Ding, M., Xue, X., Wang, Y., Zhang, C., Qiu, S., 2024. Mobilization of tight oil by spontaneous imbibition of surfactants. Pet. Sci. 21, 4176–4188. https://doi.org/10.1016/j.petsci.2024.08.010.
Dou, L., Xiao, Y., Gao, H., Wang, R., Liu, C., Sun, H., 2021. The study of enhanced displacement efficiency in tight sandstone from the combination of spontaneous and dynamic imbibition. J. Pet. Sci. Eng. 199, 108327. https://doi.org/10.1016/j.petrol.2020.108327.
Ghanbari, E., 2015. Water Imbibition and Salt Diffusion in Gas Shales: a Field and Laboratory Study. University of Alberta.
Ghandi, E., Parsaei, R., Riazi, M., 2019. Enhancing the spontaneous imbibition rate of water in oil-wet dolomite rocks through boosting a wettability alteration process using carbonated smart brines. Pet. Sci. 16, 1361–1373. https://doi.org/10.1007/s12182-019-0355-1.
Guo, J., Li, M., Chen, C., Tao, L., Liu, Z., Zhou, D., 2020. Experimental investigation of spontaneous imbibition in tight sandstone reservoirs. J. Pet. Sci. Eng. 193, 107395. https://doi.org/10.1016/j.petrol.2020.107395.
Hou, B., Zhang, F., Wang, S., Fan, H., Wen, D., Gao, S., Tian, Y., Yang, X., He, H., Zhang, X., 2022. Mechanisms of spontaneous imbibition and wettability reversal of sandstone cores by a novel imbibition agent. Energy Fuel. 36, 1316–1325. https://doi.org/10.1021/acs.energyfuels.1c03489.
Hu, Y., Zhao, C., Zhao, J., Wang, Q., Zhao, J., Gao, D., Fu, C., 2020. Mechanisms of fracturing fluid spontaneous imbibition behavior in shale reservoir: a review. J. Nat. Gas Sci. Eng. 82, 103498. https://doi.org/10.1016/j.jngse.2020.103498.
Hu, J., Zhang, G., Jiang, P., Ge, J., Pei, H., Wang, X., 2022. Study on the chemical structure characterization and emulsification-stripping of heavy oil. J. Pet. Sci. Eng. 215. https://doi.org/10.1016/j.petrol.2022.110592.
Huang, Y., Liu, F., Kang, Y., Hu, Y., Li, L., Liu, Y., 2025. Experimental study on CO_2 Huff-n-Puff for enhanced shale oil recovery and microscopic mobilization characteristics using online NMR. Fuel 387. https://doi.org/10.1016/j.fuel.2025.134428.
Javaheri, A., Habibi, A., Dehghanpour, H., Wood, J.M., 2018. Imbibition oil recovery from tight rocks with dual-wettability behavior. J. Pet. Sci. Eng. 167, 180–191. https://doi.org/10.1016/j.petrol.2018.01.046.
Jiang, Y., Shi, Y., Xu, G., Jia, C., Meng, Z., Yang, X., Zhu, H., Ding, B., 2018. Experimental study on spontaneous imbibition under confining pressure in tight sandstone cores based on low-field nuclear magnetic resonance measurements. Energy Fuel. 32, 3152–3162. https://doi.org/10.1021/acs.energyfuels.7b03776.
Jiang, Z., Li, G., Zhao, P., Zhou, Y., Mao, Z., Liu, Z., 2023. Study on spontaneous imbibition and displacement characteristics of mixed-wet tight sandstone reservoir based on high-precision balance and NMR method. Fuel 345, 128247. https://doi.org/10.1016/j.fuel.2023.128247.
Jiang, R., Tan, F., Yang, X., Luo, G., Jing, Y., Tan, L., Zhang, J., Lu, Y., Chen, K., 2025. CO_2 geological storage using different oil displacement methods in tight conglomerate reservoir samples from the Mahu depression. Energy Fuel. 39, 12581–12596. https://doi.org/10.1021/acs.energyfuels.5c00680.
Kathel, P., Mohanty, K.K., 2013. Wettability alteration in a tight oil reservoir. Energy Fuels 27, 6460–6468. https://doi.org/10.1021/ef4012752.
Le Van, S., Khishvand, M., Akbarabadi, M., Piri, M., Nagarajan, N., 2025. Oil recovery from tight reservoirs during natural depletion and cyclic gas injection: An experimental study using live fluids on a fractured reservoir whole core sample. Energy Fuel. 39, 3407–3421. https://doi.org/10.1021/acs.energyfuels.4c05329.

Li, B., Zhu, W., Ma, Q., Li, H., Kong, D., Song, Z., 2022. Pore-scale visual investigation on the spontaneous imbibition of surfactant solution in oil-wet capillary tubes. Energy Sources, Part A Recover. Util. Environ. Eff. 44, 3395–3405. https://doi.org/10.1080/15567036.2020.1849454.

Liu, Y., Wang, H., Xu, H., Guo, D., Li, M., 2023. Experimental study on characteristics of water imbibition and ion diffusion in shale reservoirs. Geoenergy Sci. Eng. 229, 212167. 10.1016/j.geoen.2023.212167.

Liu, C., Wang, T.R., You, Q., Du, Y.C., Zhao, G., Dai, C.L., 2024. The effects of various factors on spontaneous imbibition in tight oil reservoirs. Pet. Sci. 21, 315–326. https://doi.org/10.1016/j.petsci.2023.09.022.

Liu, J., Zhang, D., Liu, S., Gong, R., Wang, L., 2025. Multiscale investigation into EOR mechanisms and influencing factors for CO_2-WAG injection in heterogeneous sandy conglomerate reservoirs using NMR technology. Pet. Sci. 22, 2977–2991. https://doi.org/10.1016/j.petsci.2025.04.004.

Lv, Q., Hou, J., Cheng, Z., Chen, J., Ji, Y., Lv, J., Song, Y., Wei, J., Yang, Y., 2025. Wettability and imbibition mechanism of the multiscale pore structure of Jiyang shale oil formation by NMR. Energy Fuel. https://doi.org/10.1021/acs.energyfuels.4c05750.

Ma, J., Xiao, P., Wang, P., Han, X., Luo, J., Shi, R., Wang, X., Song, X., Zhao, S., 2022. Molecular dynamics simulation study on π-π stacking of Gemini surfactants in oil/water systems. Chin. J. Chem. Eng. 50, 335–346. https://doi.org/10.1016/j.cjche.2022.06.010.

Manshad, A.K., Mobaraki, M., Ali, J.A., Abdulrahman, A.F., Jaf, P.T., Bahraminejad, H., Akbari, M., 2024. Biphasic interfacial functioning improvement using naturally derived Hop and dill surfactants in carbonate reservoirs. J. Environ. Chem. Eng. 12, 112365. https://doi.org/10.1016/j.jece.2024.112365.

Mehana, M., Al Salman, M., Fahes, M., 2018. Impact of salinity and mineralogy on slick water spontaneous imbibition and formation strength in shale. Energy Fuel. 32, 5725–5735. https://doi.org/10.1021/acs.energyfuels.7b03516.

Nowrouzi, I., Khaksar Manshad, A., Mohammadi, A.H., 2020. Effects of TiO_2, MgO and γ-Al_2O_3 nano-particles on wettability alteration and oil production under carbonated nano-fluid imbibition in carbonate oil reservoirs. Fuel 259, 116110. https://doi.org/10.1016/j.fuel.2019.116110.

Paria, S., Khilar, K.C., 2004. A review on experimental studies of surfactant adsorption at the hydrophilic solid-water interface. Adv. Colloid Interface Sci. 110, 75–95. https://doi.org/10.1016/j.cis.2004.03.001.

Ren, W., Ma, C., Huang, X., Gu, W., Chen, Y., Liu, X., 2023. Dynamic and static imbibition characteristics of tight sandstone based on NMR. Geoenergy Sci. Eng. 229, 212052. https://doi.org/10.1016/j.geoen.2023.212052.

Santanna, V.C., Castro Dantas, T.N., Borges, T.A., Bezerril, A.R., Nascimento, A.E.G., 2014. The influence of surfactant solution injection in oil recovery by spontaneous imbibition. Petrol. Sci. Technol. 32, 2896–2902. https://doi.org/10.1080/10916466.2014.921200.

Saputra, I.W.R., Park, K.H., Zhang, F., Adel, I.A., Schechter, D.S., 2019. Surfactant-assisted spontaneous imbibition to improve oil recovery on the Eagle Ford and Wolfcamp shale oil reservoir: laboratory to field analysis. Energy Fuel. 33, 6904–6920. https://doi.org/10.1021/acs.energyfuels.9b00183.

Standnes, D.C., Austad, T., 2000. Wettability alteration in chalk 2. Mechanism for wettability alteration from oil-wet to water-wet using surfactants. J. Pet. Sci. Eng. 28, 123–143. https://doi.org/10.1016/s0920-4105(00)00084-x.

Sun, Y., Gao, K., Yu, Z., Fang, Y., Chang, Y., Chen, A., Dai, C., Wang, C., Chen, C., Xu, Y., 2020. Dynamic imbibition with aid of surfactant in tight oil fracture network model. J. Pet. Sci. Eng. 193, 107393. https://doi.org/10.1016/j.petrol.2020.107393.

Tan, M., Mao, K., Song, X., Yang, X., Xu, J., 2015. NMR petrophysical interpretation method of gas shale based on core NMR experiment. J. Pet. Sci. Eng. 136, 100–111. https://doi.org/10.1016/j.petrol.2015.11.007.

Tang, Y., Wang, R., Li, Z., Cui, M., Lun, Z., Lu, Y., 2019. Experimental study on spontaneous imbibition of CO_2-rich brine in tight oil reservoirs. Energy Fuel. 33, 7604–7613. https://doi.org/10.1021/acs.energyfuels.9b01621.

Tian, W., Lu, S., Zhang, J., Gao, Y., Huang, W., Wen, Z., Li, J., Li, J., 2022. NMR characterization of fluid mobility in low-permeability conglomerates: an experimental investigation of spontaneous imbibition and flooding. J. Pet. Sci. Eng. 214, 110483. https://doi.org/10.1016/j.petrol.2022.110483.

Wang, F., Cheng, H., Song, K., 2021. A mathematical model of surfactant spontaneous imbibition in a tight oil matrix with diffusion and adsorption. Langmuir 37, 8789–8800. https://doi.org/10.1021/acs.langmuir.1c01139.

Wang, F., Wang, L., Jiao, L., Liu, Z., Yang, K., 2023. Experimental mechanism for enhancing oil recovery by spontaneous imbibition with surfactants in a tight sandstone oil reservoir. Energy Fuels 37, 8180–8189. https://doi.org/10.1021/acs.energyfuels.3c00525.

Xiao, L., Mao, Z., Zou, C., Jin, Y., Zhu, J., 2016. A new methodology of constructing pseudo capillary pressure (Pc) curves from nuclear magnetic resonance (NMR) logs. J. Pet. Sci. Eng. 147, 154–167. https://doi.org/10.1016/j.petrol.2016.05.015.

Xiao, W., Yang, Y., Li, M., Li, N., You, J., Zhao, J., Zheng, L., Zhou, K., Ren, J., Wang, Y., 2021. Experimental study on the oil production characteristics during the waterflooding of different types of reservoirs in Ordos Basin, NW China. Petrol. Explor. Dev. 48, 935–945.

Xiao, L., Hou, J., Wen, Y., Qu, M., Wang, W., Wu, W., Liang, T., 2022. Imbibition mechanisms of high temperature resistant microemulsion system in ultra-low permeability and tight reservoirs. Petrol. Explor. Dev. 49, 1398–1410. https://doi.org/10.1016/S1876-3804(23)60358-1.

Xiao, Y., You, Z., He, Y., Du, Z., Zheng, J., Wang, L., 2025. Capillary-dominated imbibition in heterogeneous-wet reservoirs: mechanisms, characterizations, and critical insights. Geoenergy Sci. Eng. 246, 213606. https://doi.org/10.1016/j.geoen.2024.213606.

Xie, K., Wu, Z., Liu, C., Mei, J., Cao, W., Ding, H., Zhang, X., Xu, H., Suo, Y., Tian, X., Lu, X., 2024. A review of mechanisms and ML-based research on factors affecting spontaneous imbibition of surfactant. Geoenergy Sci. Eng. 240, 213071. https://doi.org/10.1016/j.geoen.2024.213071.

Xiong, Y., Li, S., Li, M., Leng, A., Chen, M., Deng, B., Yu, K., 2025. Study on characteristics of imbibition and recovery predicted methods with different lithology structure. Fuel 381, 133525. https://doi.org/10.1016/j.fuel.2024.133525.

Xu, R., Yang, S., Xiao, Z., Jin, Y., 2022. Quantitatively study on imbibition of fracturing fluid in tight sandstone reservoir under high temperature and high pressure based on NMR technology. J. Pet. Sci. Eng. 208, 109623. https://doi.org/10.1016/j.petrol.2021.109623.

Xu, N., Wang, Y., Zhang, C., Bai, B., Li, D., Zhang, Y., 2025. Effect of surfactants on the interface characteristics and imbibition processes in shale oil reservoirs. Colloids Surf., A Physicochem. Eng. Asp. 706, 135818.

Yan, L., Raoof, A., An, S., 2025. Impact of salinity on spontaneous emulsification near water/oil interfaces. Earth Energy Sci. 1, 228–241. https://doi.org/10.1016/j.ees.2025.07.003.

Yang, L., Ge, H., Shi, X., Cheng, Y., Zhang, K., Chen, H., Shen, Y., Zhang, J., Qu, X., 2016. The effect of microstructure and rock mineralogy on water imbibition characteristics in tight reservoirs. J. Nat. Gas Sci. Eng. 34, 1461–1471. https://doi.org/10.1016/j.jngse.2016.01.002.

Yang, L., Wang, H., Xu, H., Guo, D., Li, M., 2023. Experimental study on characteristics of water imbibition and ion diffusion in shale reservoirs. Geoenergy Sci. Eng. 229, 212167. https://doi.org/10.1016/j.geoen.2023.212167.

Yang, K., Wang, F., Zhao, J., 2023a. Experimental study of surfactant-enhanced spontaneous imbibition in fractured tight sandstone reservoirs: The effect of fracture distribution. Pet. Sci. 20 (1), 370–381. https://doi.org/10.1016/j.petsci.2022.09.033.

Yang, Y., Hu, Y., Zhu, Y., Zhang, J., Song, P., Qin, M., Wu, H., Song, Z., Hou, J., 2023b. Similarity-based laboratory study of CO_2 huff-n-puff in tight conglomerate cores. Pet. Sci. 20 (1), 362–369. https://doi.org/10.1016/j.petsci.2022.09.030.

Yekeen, N., Padmanabhan, E., Idris, A.K., Ibad, S.M., 2019. Surfactant adsorption behaviors onto shale from Malaysian formations: Influence of silicon dioxide nanoparticles, surfactant type, temperature, salinity and shale lithology. J. Pet. Sci. Eng. 179, 841–854. https://doi.org/10.1016/j.petrol.2019.04.096.

Yildiz, H.O., Gokmen, M., Cesur, Y., 2006. Effect of shape factor, characteristic length, and boundary conditions on spontaneous imbibition. J. Pet. Sci. Eng. 53, 158–170. https://doi.org/10.1016/j.petrol.2006.06.002.

Zhang, T., Li, Z., Gao, M., Xu, Z., Adenutsi, C.D., You, Q., 2022a. New insights into the synergism between silica nanoparticles and surfactants on interfacial properties: Implications for spontaneous imbibition in tight oil reservoirs. J. Pet. Sci. Eng. 215 (5), 110647. https://doi.org/10.1016/j.petrol.2022.110647.

Zhang, T., Li, Z., Adenutsi, C.D., Wei, Y., Ma, Z., You, Q., 2022b. Quantitative investigation of nanofluid imbibition in tight oil reservoirs based on NMR technique. Pet. Sci. 19 (5), 2185–2198. https://doi.org/10.1016/j.petsci.2022.04.013.

Zhang, P., Wang, R., Liu, S., Mu, Z., Chen, J., Xiu, Q., Wei, Q., Tian, S., 2025. Characteristics and influencing factors of spontaneous imbibition in deep tight conglomerate reservoirs in the Mahu Sag. Sci. Rep. 15, 37608. https://doi.org/10.1038/s41598-025-21543-z.

Zheng, H., Liao, R., Cheng, N., Shi, S., 2021. Microscopic mechanism of fracturing fluid imbibition in stimulated tight oil reservoir. J. Pet. Sci. Eng. 202, 108533. https://doi.org/10.1016/j.petrol.2021.108533.

Zhigarev, V.A., Pryazhnikov, M.I., Skorobogatova, A.D., Pryazhnikov, A.I., Minakov, A.V., Zharkov, S.M., 2025. Comparing the effect of nanofluids in capillary imbibition with traditional displacing fluids. Pet. Res. https://doi.org/10.1016/j.ptlrs.2025.01.004.

Zhou, X., Yuan, Q., Zhang, Y., Wang, H., Zeng, F., Zhang, L., 2019. Performance evaluation of CO_2 flooding process in tight oil reservoir via experimental and numerical simulation studies. Fuel 236, 730–746. https://doi.org/10.1016/j.fuel.2018.09.035.

Zhou, X., Li, X., Shen, D., Shi, L., Zhang, Z., Sun, X., Jiang, Q., 2022. CO_2 huff-n-puff process to enhance heavy oil recovery and CO_2 storage: An integration study. Energy 239, 122003. https://doi.org/10.1016/j.energy.2021.122003.

Zhou, X., Li, H., Zeng, F., Yu, C., Ouyang, H., Jiang, Q., 2025. Lightning of shale oil using high-temperature supercritical CO_2: An experimental study. Adv. Geo-Energy Res. 16 (2), 99–113. https://doi.org/10.46690/ager.2025.05.03.